Defence Science Journal, Vol. 62, No. 3, May 2012, pp. 187-192, DOI: 10.14429/dsj.62.843

Ultra-wideband Impulse-based Radar Signals for Through-the-wall Imaging

Puli Kishore Kumar* and T. Kishore Kumar
National Institute of Technology, Warangal-506 004, India
**E-mail: pulikishorek@nitw.ac.in*

ABSTRACT

Ultra-wideband (UWB) is the promising technology for localization of the objects behind the walls. Recent terrorist activities and law-enforcement situations underscore the need for effective through-wall detection. The approval of UWB technology made by federal communications commission (FCC) in 2002 makes the researchers to have a look on this technology. UWB radar signals has extremely large frequency spectrum and since low frequencies has more penetration capabilities through dielectric materials it is best suitable for through-the-wall radar imaging (TWRI). Signal processing in TWRI has a greater impact in getting the information of the scanned area. This paper uses impulse signals in TWRI, examines the factors impacting in TWRI and obtains the two dimensional information of the scanned scene. Electromagnetic simulation software is used to generate the room like structure, and to obtain the raw radar data.

Keywords: Ultra-wideband, impulse signal, through-the-wall imaging, through-the-wall radar imaging, synthetic aperture

1. INTRODUCTION

The field of remote sensing has developed a range of interesting imaging approaches for a variety of applications. Through-the-wall and through-the-building sensing are relatively new areas that address the desire to see inside structures to determine the layout of buildings, where occupants may be, and even identify materials within the building. Through-wall sensing is highly desired by police, fire and rescue, emergency relief workers, and military operations. Accurate sensing and imaging can allow a police force to obtain an accurate description of a building in a hostage crisis, or allow firefighters to locate people trapped inside a burning building. The goals of through-the-wall sensing technology are to provide vision into otherwise obscured areas.

Each remote-sensing application area has driven different sensing modalities and imaging algorithm development based upon propagation characteristics, sensor positioning, and safety issues. Traditional optical, radar, and sonar image processing all begin with basic wave physics equations to provide focusing to individual points. In many radar applications, for example, data sampled from many sensors are mathematically integrated to provide equivalent focusing using free-space propagation assumptions. Free-space imaging is commonly seen in synthetic aperture radar (SAR) techniques1 since atmospheric distortions are often negligible and can be safely ignored in first-order calculations.

Free-space propagation does not apply for many interesting applications like geophysical sensing, medical imaging, and more recently through building sensing where transmission through scattering media is encountered. In these applications, propagated signals diffract through a volume. As examples, geophysical imaging techniques generally measure seismic propagation through the earth to look for discontinuities that are often indicators of oil, gas, water, or mineral deposits. In medical imaging, ultrasound tomography approaches account for propagation through different tissue classes 2.

Non-free-space scattering applications are more representative of the through-building sensing problem, albeit each has its own distinct challenges and approaches. In through-building sensing, there are many air–material interfaces that dramatically change the wave front. Through building sensors may be located some distance away from the structure and attenuation is largely seen only in the building materials and contents rather than in the large volumes of air that occupy most of the space within a building. Sensor standoff provides unique opportunities and challenges for exploiting building-dependent features.

2. MEASUREMENT SCENARIO

A simplified sketch of the topview of measurement layout is shown in Fig 1. The radar system was horizontally scanned parallel to the front brick wall at a distance of 43.75 cm from the wall as shown in figure. The positions are represented as a1- a9, (i.e., a1, a2, a3… a9). The wall is considered as the brick wall and the specifications are given in Table 1. The side view and the orthographic view of the simulated scene is shown in Figs 2 and 3.

The area that is scanned behind the wall covers the volume of 800 cm × 700 cm × 500 cm indicates length,

Received 23 February 2011, revised 07 April 2012, online published 3 May 2012

Table 1. Electrical Parameters of the brick wall

Type of wall	Brick wall
Relative permittivity	4.440
Conductivity	0.001 S/m
Thickness of the wall	0.125 m

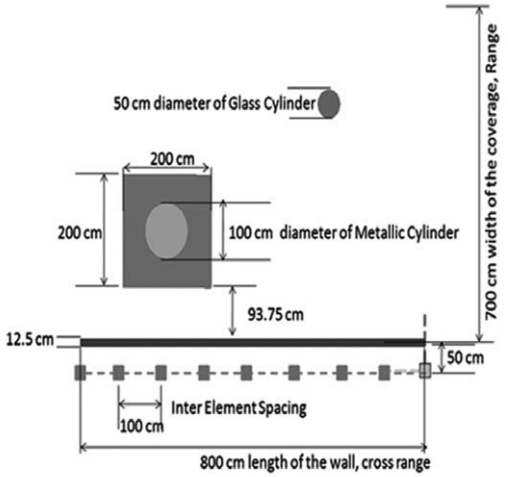

Figure 1. Top view of the simulated measurement scenario.

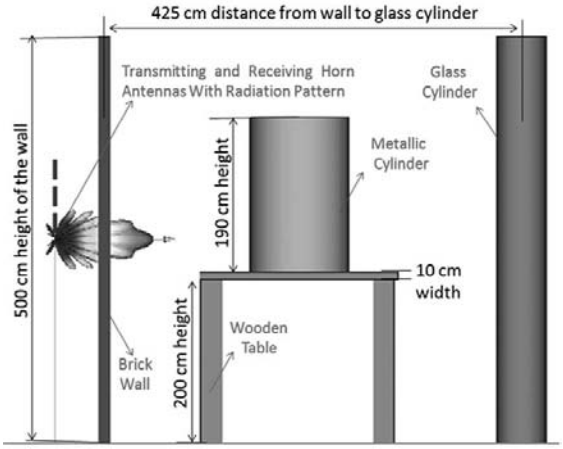

Figure 2. Side view of the simulated measurement scenario.

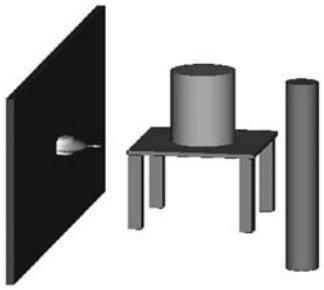

Figure 3. Orthographic view.

width and height respectively. The transmitting and the receiving antennas are placed at the same position, keeping in view to make use of the same antenna for both transmitting and receiving for further studies. The objects that were placed behind the wall consists a wooden

Table 2. Wooden table and properties glass cylinder properties

Properties	Wooden table	Glass cylinder
Thickness(m)	0.100	0.003
Roughness	0.000	0.000
Conductivity	0.000000	0.000000
Permittivity	5.000000	2.400000

table on which an iron cylinder is placed and at other position a glass cylinder is placed. The specifications of the wooden table, iron cylinder and glass cylinder are given in Table 2.

One reason of selecting these materials (wood, metal and glass) is to check how the reflection of the signals takes place, and the second is these materials usually found in any rooms.

The term ultra-wideband refers to electromagnetic signal waveforms that have instantaneous fractional bandwidths greater than 0.25 with respect to a center frequency. The fractional bandwidth is given by 3, 4, 5, 20,23.

$$fractional\ bandwidth = \frac{f_H - f_L}{f_c} \quad (1)$$

$$f_c = \frac{f_H + f_L}{2}$$

where f_H, f_L, are the higher and lower 10 dB frequencies and f_c is the center frequency.

The federal communications commission (FCC) emission limit for UWB-based through-wall imaging devices is shown in Fig. 4[6,25]. This mask is used to avoid interference with existing communication systems. The operation of these devices is constrained to law enforcement and rescue teams.

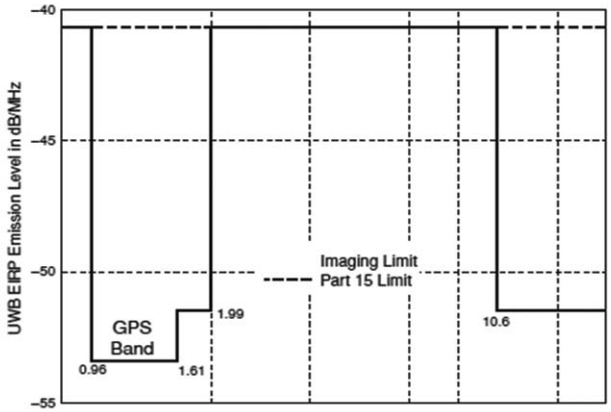

Figure 4. UWB emission limits for through-wall imaging.

Since Ultra-Wideband (UWB) signals have better penetration properties[12] and has the capability of obtaining high resolution images, we use an impulse signals particularly Gaussian derivative is used. The resolution is proportion to the bandwidth of the signal[3,4] and is

given by

$$\Delta R = \frac{c\tau}{2} = \frac{c}{2B} \quad (2)$$

where ΔR is range resolution, τ is pulse width, and B is bandwidth and c = 3×108 m/sec is the velocity of light in free space.

The reason of selecting Gaussian doublet or the second derivative of the Gaussian pulse for transmitting is that it has only one peak which can be easily noticed in the time domain and also has the longest lobe in the frequency domain, creating the large bandwidth of the signal. Another pulse would not fit these requirements since it would not have both the large single pulse in the time domain and cover a large spectrum in the frequency domain7, 8. Other waveforms like noise like waveforms 9, 10, 11, 13, 16, 21, 22, 24 multi band OFDM signals, stepped frequency signals also meets FCC limits of UWB technology but is out of scope for this article.

Since the signal transmitted by the antenna is the derivative of the input signal, to make use of Gaussian doublet Gaussian first derivative is given as input signal to the antenna. The expressions for Gaussian pulse and its derivatives (up to second order derivative) are given by

$$f(t) = A\exp(-\frac{t^2}{2\tau^2})$$

$$f'(t) = -\frac{At}{\tau^2}\exp(-\frac{t^2}{2\tau^2})$$

$$f''(t) = -\frac{A}{\tau^2}(1-\frac{t^2}{\tau^2})\exp(-\frac{t^2}{2\tau^2}) \quad (3)$$

The signal that was used here has the pulse width of 0.5 ns and the with centre frequency of 1.83 GHz and 3.3 GHz bandwidth. The plot of the Gaussian derivative and its spectrum is shown in Fig. 5.

Horn antennas were used for transmission and reception. Selecting horn antenna enhances the gain in the direction of scanning and to not to considering the region behind the antenna which is of no use. The horn antenna specifications and its radiation pattern are shown in Fig. 6.

3. EFFECT OF ANTENNA CROSSTALK AND RANGE GATING IN TWRI

Crosstalk is the part of the signal that travels directly between the transmitting and receiving antennas. It is the first and often the largest peak in the A-scan signal which affects the mean value of the signal. This signal is constantly present in all the measurements and contains no information of the scanned scene. Sometimes this largest peak signal may cross the maximum current rating of the receiver circuit over which the performance may be degraded 8. Hence it is very important to remove the crosstalk. The crosstalk can be obtained by measuring with radar in the free space, or with absorbers around (anechoic chamber). The A-Scan signal after crosstalk removal is given by

$$A_{pcr}(n) = A_p(n) - c_p(n) \quad (4)$$

where $A_p(n)$ and $c_p(n)$ are the A-scan signal and crosstalk at pth position of an antenna respectively and $A_{pcr}(n)$ represents the A-scan signal at pth position with crosstalk removed. Figure 7 shows the waveforms of crosstalk, A-scan signal at 'a_1' position with and without crosstalk removal.

Range gating is the basic preprocessing technique that decides to fix the maximum range of the scanned area. The receiver is made to switch on up to the delay that was fixed by the maximum range. After that delay the signal is assumed to be of even farther distance and hence ignored. The delay that was obtained for 500cm range is 0.466×10^{-9} s. Since the velocity inside the wall is gets reduced by a factor of $\sqrt{\mu_r\varepsilon_r}$ the delay was increased to 0.55×10^{-9} s which occurs at the index of 110000th sample.

Figure 8(a) shows the received A-scan signal at 'a_1' position and Fig. 8(b) shows the range gated signal. The reader should note that the multiplication factor of time

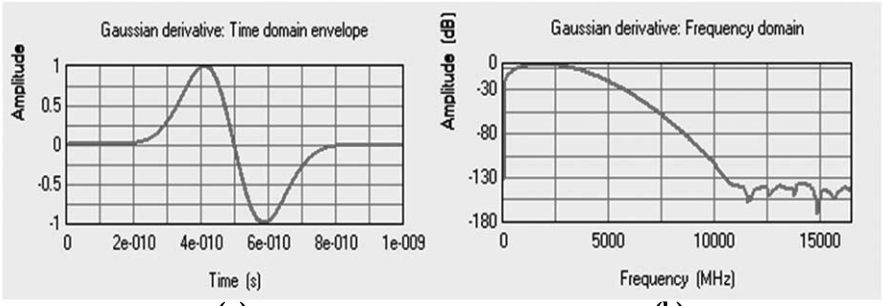

(a) **(b)**

Figure 5. (a) Gaussian derivative and (b) frequency spectrum.

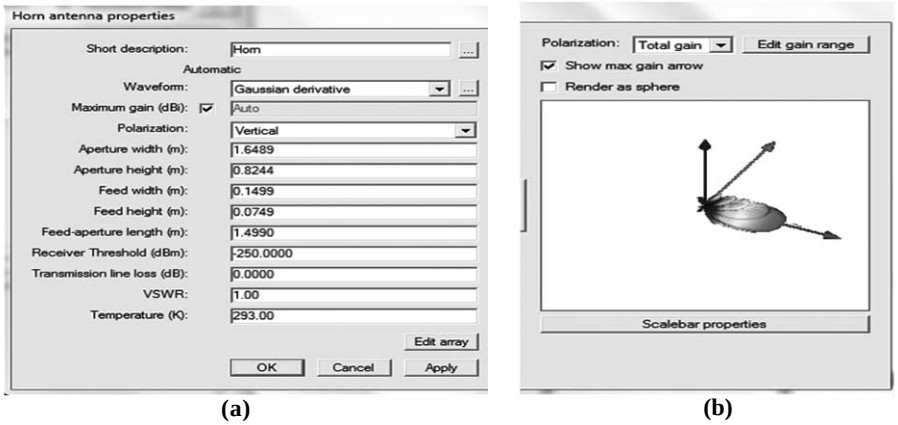

(a) **(b)**

Figure 6. (a) Specifications of horn antenna and (b) Horn antenna radiation pattern.

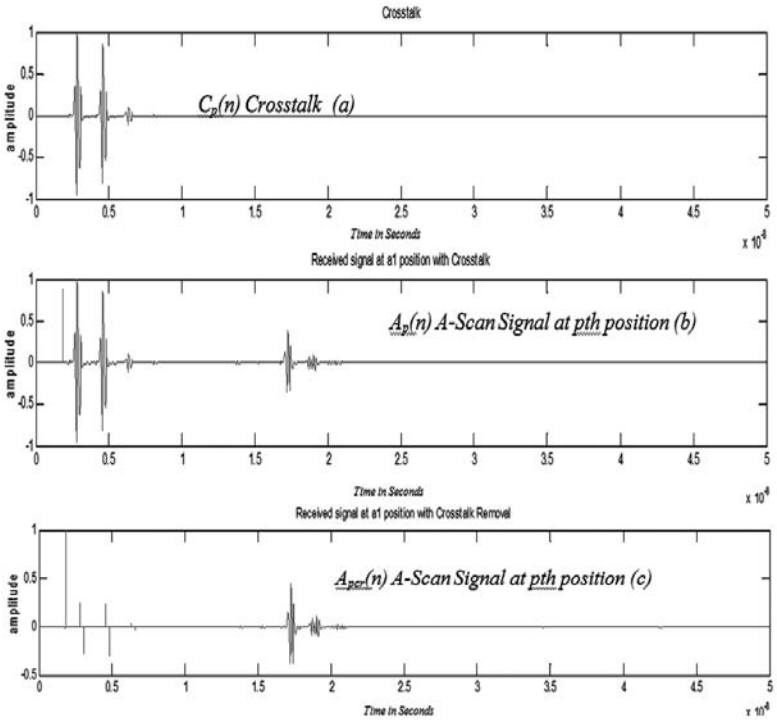

Figure 7. (a) Crosstalk measurement, (b) received A-scan signal, and (c) A-scan signal after removing the crosstalk.

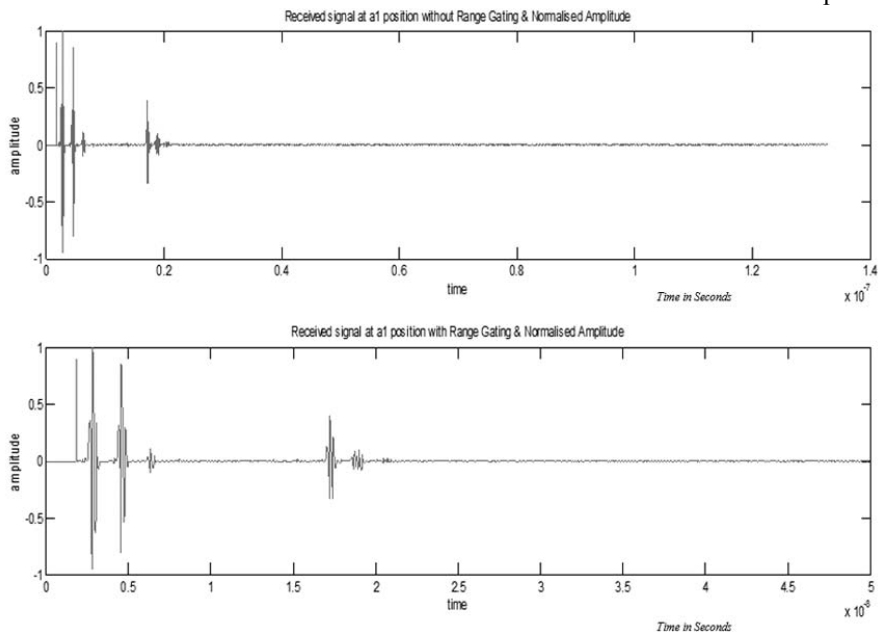

Figure 8. (a) A-scan signal without range gating, (b). A-scan signal with range gating.

is 10^{-7} for Fig. 8(a) and 10^{-8} for Fig. 8(b). This coincides with the calculated to 0.55×10^{-9} s.

4. BACK PROJECTION ALGORITHM

Back projection algorithm is used in many applications to retrieve images, particularly in ground penetrating radar for landmine detection and imaging, synthetic aperture radar for imaging the scanned region14, 15, 16,17, 18, 19.

This algorithm retrieves the image of the scanned area by making use of the A-scan signals at different receiver positions. Since the image is of 2D and is represented by an $M\times N$ matrix, the aim is obtain the corresponding numerical values to fill the matrix, such that the formed image should represent the scanned scene. Each numerical value in the $M\times N$ matrix represents a pixel value of an image. This image or 2D signal is also called as B-scan signal[11].

The numerical value at any pixel position should be the contribution of the A-scan signals at all receiver positions. Since the range is fixed to 700 cm and the number of pixels in the range direction is N (N represents cross range and M represents the range), the range bins are selected such that the maximum range should not cross the prescribed value.

The A-scan signal received at each receiver position assuming P targets in the region is represented as 9,10

$$A_i(t) = \sum_{j=1}^{P} a_{ij} s(t - t_{ij}) \tag{5}$$

where $A_i(t)$ is the A-scan signal at i^{th} receiver position, a_{ij} is the reflection coefficient of the jth tatget and t_{ij} is the delay of the signal from i^{th} transmitter position to j^{th} tatget position and to i^{th} receiver position and is given by

$$t_{ij} = \frac{2R_{ij}}{c} \tag{6}$$

where R_{ij} is the distance from ith transmitter position to the j^{th} target position.

A weight factor also should be there in Eqn (5) representing the attenuation of the signal. Similarly a term should be added in Eqn (6) representing the reduction of velocity inside the wall. Since the intention is to obtain the image, these terms are given little importance in this paper.

The point spread response (PSR) which represents the spreading of signal energy in two dimensional space of a given A-scan signal is given by

$$f_p(x_i, y_j) = A_p(t - \tau(x_i, y_j)) \tag{7}$$

where i= 0,1,2,3…..M

j= 0,1,2,3…..N

(x_i, y_j) : Pixel Coordinates

and $\mathrm{t}(x_i, y_j)$ is the focusing delay 9 in the image space. The PSR at a1th receiver position is shown in Fig. 9.

But the final image should have the contribution of all A-scan signals and hence all the PSR should be added. The expression is given by

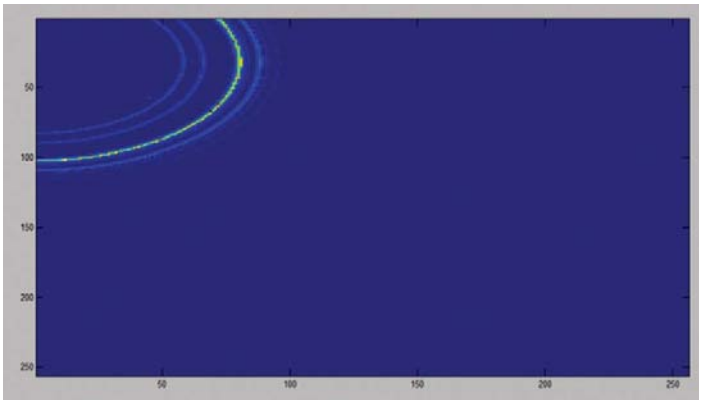

Figure 9. Point spread response.

$$B(x_i, y_i) = \sum_{p=1}^{L} f_p(x_i, y_i) \tag{8}$$

5. RESULTS

Computer simulations implementing the impulse signals for through the wall imaging is done. The back projection algorithm is used to retrieve the image of the scanned region and the results obtained are shown in Figs 10 and 11. The data collected from the receivers at different receiver positions is used in MATLAB to implement the algorithm.

Results clearly demonstrates the position of the objects

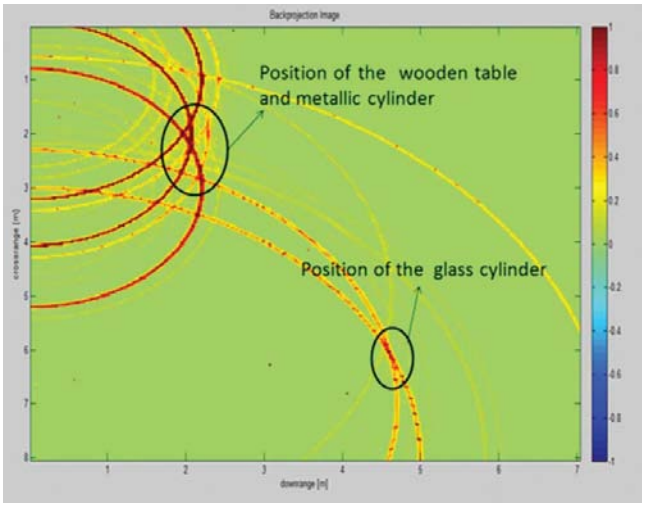

Figure 10. Two dimensional image of the scene without wall indicating the position of the objects.

that were there in the scanned region. The intersection point of the point spread responses obtained for different receiver position indicates the presence of the object. It can be observed from Fig. 11 that the position of class cylinder is not visible. This is because of the less reflection coefficient of the glass compared to the metallic cylinder. Since our aim is to identify all types of targets this is a drawback for present simulation. Time varying gain of the A-scan signal is to be included so as to rectify this issue. This can be considered as the future scope of the work.

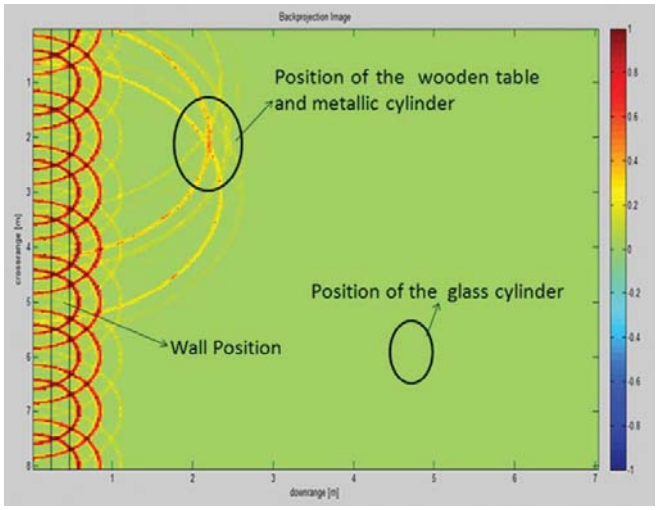

Figure 11. B-scan image of the scene with wall.

6. CONCLUSIONS

An approach of making use of impulse based signals for through the wall imaging is presented. Electromagnetic simulation software is used to model the wall and objects inside the room. Three different materials were selected. The need for removing crosstalk and the necessasity of range gating is also explained. Finally back projection algorithm is analysed and used in retrieving the two dimensional image of the scanned region.

REFERENCES

1. Franceschetti, Giorgio & Lanari, Riccardo. Synthetic aperture radar processing. CRC Press, New York, 1999.
2. Kak, A.C. & Slaney, M. Principles of computrized tomographic imaging. IEEE Press, New York, 1988.
3. Taylor, James D. Ultra-wide band radar technology. CRC Press, New York, 2001
4. Taylor, J.D. Introduction to ultra-wideband radar systems. CRC Press, Boca Raton, FL.
5. http://www.uwbgroup.ru/eng/common/(Accessed on 01/07/2009)
6. Ambors, M. Ultra-wideband radar seeing through walls. A project report submitted to United States Coast Guard Academy, USA, 2007
7. Safaai-Jazi, Ahmad; Riad, Sedki M.; Muqaibel, Ali & Bayram, Ahmet. Ultra-wideband propagation measurements and channel modeling. DARPA NETEX Time Domain and RF Measurement Laboratory, Virginia, November 18, 2002.
8. Gauthier, Sylvain & Chamma, Walid. Through–the–wall surveillance. Technical Memorandum, DRDC Ottawa, Canada, October 2002.
9. Withington, P. & Fullerton, L. An impulse radar communications system. *In* Ultra-Wideband, Short-Pulse Electromagnetics, Plenum Press, 1993 pp.113-20.
10. Greg Barrie. Ultra-wideband Synthetic Aperture. Technical Memorandum, DRDC Ottawa, Canada,January 2003.

11. Aftanas, Michal. Through the wall imaging using M-sequence UWB radar system. Slovak. Republic. December 2007. (PhD Thesis)
12. Barrie, Greg. Ultra-wideband synthetic aperture. data and image processing. Technical Memorandum, DRDC Ottawa, January 2003.
13. Thanh, N.T.; Kempen, L. van; Savelyev, T.G.; Zhuge, X.; Aftanas, M.; Zaikov, E.; Drutarovsky, M. & Sahli, H. Comparision of basic inversion techniques for through-wall imaging using UWB Radar. *In* Proceedings of 5th European Radar Conference, Amsterdam, Netherlands. October 2008. pp 140-143.
14. Ahmad, Fauzia; Amin, Moeness G.; Saleem & Kassam, A. Synthetic aperture beamformer for imaging through a dielectric wall. *IEEE Trans. Aero. Electr. Syst.*, 2005, **41**(1), 271-82.
15. Yang, Y. E. & Pathy, A. E. See the through the wall imaging using UWB short pulse radar system. Antennas and propagation international symposium, Knoxville, USA. July 2005. pp 334-37.
16. Venkatasubramanian, V. & Leung, H. A Novel Chaos based high resolution imaging technique and its application to the through the wall imaging. IEEE Signal Processing Letters, 2005, **12**(7), 528-31.
17. Ahmed, Ishtiaque. Study of local back projection algorithm for image formation in ultra wideband synthetic aperture radar. Blekinge Institute of Technology, December 2008.
18. Daniels, David J. Ground penetrating radar. The Institution of Electrical Engineers, UK, 2004.
19. Daniels, D.J. Surface-penetrating radar. *In* IEE Radar, Sonar, Navigation and Avionics Series 6, 1996, 300 p.
20. Immoreev, I. Moscow aviation institute about UWB. *IEEE Aero. Elect. Syst. Mag.*, 2003. **18**(11), 8-10.
21. Mahafza, Bassem R. & Elsherbeni, Atef Z. MATLAB simulations for radar systems design. CRC Press, New York, 2004.
22. Aftanas, Michal. Through the wall Imaging using M-sequence UWB radar system. Department of Electronics and Multimedia Communications, Technical University at Kosice, Slovak Republic. December 2007. (PhD thesis)
23. Gauthier Sylvain, Eric Hung & Chamma Walid. Surveillance Through Concrete walls. Technical Memorandum, DRDC Ottawa, Canada, December 2003.
24. Venkatasubramanian, V. Chaos UWB Radar for Through-the-Wall Imaging. *IEEE Trans. Image Processing*, 2009, **18**(6), 1255-265.
25. Ghavami, M.L.; Michael, B. & Kohno, R. Ultra wideband signals and systems in communication Engg. Wiley 2007.

Contributors

Mr Puli Kishore Kumar received MTech (Communication & Radar Systems) and BTech (Electronics & Communication) Engineering from Koneru Lakshamaiah University, Guntur. He is a research scholar from National Institute of Technology (NIT), Warangal. He has published 5 research articles in various international conferences & journals.

Dr T. Kishore Kumar received PhD from Jawaharlal Nehru Technological University, Hyderabad. Presently working as Associate Professor in Department of Electronics & Communication Engineering, NIT, Warangal. At present he is guiding 4 PhD Scholars and 4 MTech Students. He has published 19 papers in the international journals and conferences. He is the Member of IEEE and also member of IETE. His areas of interest are signal processing and speech processing.